

EDINBURGH
INSTRUMENTS



PRECISION RAMAN

Best-in-class Raman microscopes
for research and analytical requirements
backed with world-class customer
support and service.



edinst.com

Glaze characterization of the glazed pottery from the medieval workshop of Vega (Burgos, Spain)

Ainhoa Alonso-Olazabal¹  | Luis Angel Ortega¹  | Maria Cruz Zuluaga¹  |
Carmen Alonso-Fernández² | Javier Jimenez-Echevarría² | Alfredo Sarmiento³

¹Geology Department, University of Basque Country UPV/EHU, Leioa, Bizkaia, Spain

²Cronos S.C. Arqueología y Patrimonio, Burgos, Spain

³LASPEA unit from the Advanced Research Facilities (SGIker), University of Basque Country UPV/EHU, Leioa, Bizkaia, Spain

Correspondence

Ainhoa Alonso-Olazabal, Geology Department, Science and Technology Faculty, University of the Basque Country UPV/EHU, Campus of Leioa, Sarriena s/n, 48940 Leioa, Bizkaia, Spain.
Email: ainhoa.alonso@ehu.eus

Funding information

Basque Country Government, Grant/Award Number: IT1193-19

Abstract

Sixteen glazes on medieval (14th–16th century AD) pottery fragments from Vega pottery workshop (Burgos, Spain) were characterized to investigate the production technology. To this end, Raman spectroscopy and scanning electron microscopy coupled with energy dispersive X-ray spectroscopy (SEM-EDX) were used. The studied glaze samples correspond to fragments of high-quality glazed ware used by the wealthiest society in the city of Burgos. The most representative types of glazes, corresponding to honey-marble, honey-yellow, bright light green, and dark green types, were analysed. Raman spectroscopy shows lead was used as a fluxing agent in glaze production. SEM-EDX analysis confirms the use of lead oxide and evidences that most of the samples underwent at least two firing processes. No Raman signals of crystalline phases were detected on either glaze surfaces or glaze thin-sections. The exception is the single firing of dark green glazes, which show pseudobrookite and rutile at the clay body/glaze interface measured in thin section. No colouring crystalline phases were identified by Raman spectroscopy either. However, SEM-EDX shows iron was the most-used colouring agent whereas copper was used for bright light green glazes. The polymerization index (I_p) values were used to estimate the firing temperatures. The polymerization index values are typically low for lead glazes and indicate firing temperatures below 700°C.

KEYWORDS

firing temperatures, lead glazes, polymerization index, Raman spectroscopy, SEM-EDX

1 | INTRODUCTION

In recent decades, several studies of ancient ceramics have combined Raman spectroscopy and scanning electron microscopy techniques. These techniques allow the micro-characterization of different parts of the ceramic: glaze, body, body/glaze interface, opacifiers, and pigments. The information provided by these methods can

be used to elucidate several archaeological issues: provenance and the manufacturing technology of ceramics or firing conditions.

Raman spectroscopy is non-destructive and one of the most effective techniques to characterize glazes as a function of the degree of connection of the SiO_4^{-2} tetrahedra network of the vitreous amorphous matrix. This three-dimensional Si–O network can be modified by the

incorporation of other elements (M), such as lead or alkaline earth/alkali elements, and by the processing temperature. Variations of the spectral position and the relative Raman intensity of Si–O bending and stretching modes (at $\sim 500\text{ cm}^{-1}$ and 1000 cm^{-1} , respectively) can be investigated to observe the connectivity of the SiO_4 polymeric units related to glaze composition. The ratio of the bending and stretching envelope areas, defined as the polymerization index (I_p), is correlated with bulk composition and allows an estimation of the processing temperature.^[1,2] Raman spectroscopy also identifies crystalline phases generated during the firing process in the manufacture and/or formed by the weathering of the glazes both during material exposure to the weathering agents and during burial. In the case of coloured glazes, Raman spectroscopy is also appropriate for the identification of the colouring agents since they can be either formed by firing or added to the glaze mass.^[3–10] Besides, the final colour and surface effects, such as brilliancy and opacity, depend also on the method of glaze application, the composition of the ceramic body, the firing process, the pre-processing of the materials and the amount and nature of the colourants.^[11,12]

Raman spectroscopy is sometimes able to determine the colouring agent because of modifications to the polymerization of the network.^[13]

In studies of ceramic glazes, Raman spectroscopy results are complemented by SEM-EDX analyses.^[14–16] Electron microscopy is a suitable technique for the characterization of glaze microstructure and the glaze-ceramic body interface, as well as the occurrence of crystalline phases, their size, shape and chemical composition, and the presence of colouring agents.^[11,12,17–20] Hence, the combination of both analytical methods has become the standard approach to understand the production technology of glazed ceramics.

The aim of the present study was to characterize the glazes on pottery from Vega workshop (Burgos, Spain) in order to determine the chemical composition of glazes and to estimate the firing temperatures, using the combination of Raman Spectroscopy and Electron Microscope analysis.

2 | MATERIALS AND METHODS

2.1 | Archaeological overview and samples

Glazed ceramics were collected during the emergency archaeological excavation linked to urban development in the centre of Burgos (northern Spain). The studied samples come from a workshop specialized in the manufacture of glazed ceramics. The site was an important medieval workshop where glazed ceramics

were manufactured from the late 14th to the 16th centuries. Some of the first glazed ceramics manufactured in Christian territory, they replaced traditional pottery (unglazed) among the wealthiest stratum of Burgos society. According to the archaeological evidence, the workshop specialized in high-quality functional ware with very particular stylistic features (decoration and colours of glazes) that allow them to be traced geographically.

The workshop includes a waste dump where pieces that did not pass the quality control, due to either moulding or firing defects, or because of breakage, were accumulated. Thanks to the abundance of this waste dump, a wide range of the manufactured glazed products was observed. The analysed assemblage corresponds to the most representative productions, consisting mainly of bowls, plates and jars or pitchers with a glazed surface which came in three basic colours: yellow, green, and honey-colour (Table 1). Most of the samples are glazed on both sides and with different colours. Commonly the glazes do not occur as a pure single colour and a mix of two colours and/or a chromatic grading on a single surface is usually observed. Sixteen representative glazed samples were analysed. They came from different chronological periods and displayed the predominant glaze colours: honey-marbled (V0), honey-yellow (V1), bright light green (V3), dark green (V6), and honey-coloured (V9) glazes (Table 1). Thus, each V type represents a group of samples with similar glazes colours.

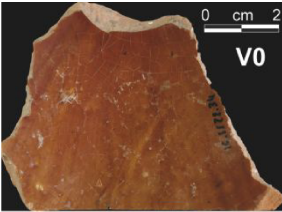

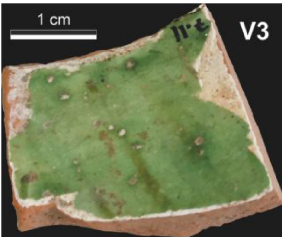
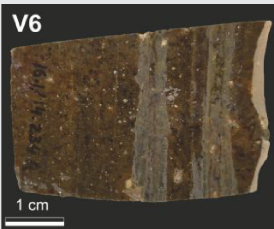
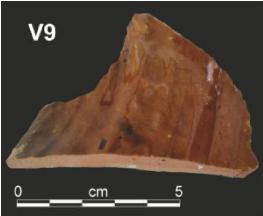
Most of the recovered fragments display a predominant dark green glazes on both on the outer and inner surfaces. Honey-marbled and honey-yellow glazes are the next most common colours, while the bright light green colour is less frequent. In some sherds, bright green-coloured glaze is observed on the outer surface and honey yellow glaze on the inner surfaces.

The glazes were applied on two types of ceramic bodies: a reddish clay body and a white one. In both cases, glazes were found to only partially cover the substrate. Another distinctive characteristic is the use of a white slip between the body and the glassy coating on reddish ceramic bodies (Table 1). This white slip promotes a depth of colour, offers a different colour than the underlying clay body, and increases the colour variety on the same ceramic piece. In addition, the use of slips increases the hardness, decreases the permeability of the body as well as being decorative.^[21–23]

2.2 | Optical microscopy observations

Macroscopic analysis was carried out on ceramic fragments using a binocular microscope (Nikon SMZ-U; 7 \times , 20 \times , and 40 \times magnifications) after washing the samples

TABLE 1 Studied ceramics grouped according to glaze colour and reporting their main characteristics

Sample	Glaze colour	Representative sample	Body colour	Slip	Chronology	Chemical group	Interface features
VE-20	Honey-marble V0		Reddish		End of 14th	Pb rich (V0)	Thinner, poor in crystallites
VE-22			Reddish		End of 14th	Pb rich(V0)	Thinner, poor in crystallites
VE-15	Honey yellow V1		Whitish		1st half of 15th	Pb rich (V1-1)	Thinner, poor in crystallites
VE-35			Reddish		2nd half of 15th	Pb rich (V1-1)	Thinner, poor in crystallites
VE-34			Reddish		1st half of 16th	Pb rich + Zn (V1-2)	Thinner, poor in crystallites
VE-18			Whitish		1st half of 15th	Pb poor + Zn (V1-3)	Thicker, rich in crystallites
VE-19			Whitish		1st half of 15th	Pb poor + Zn (V1-3)	Thicker rich in crystallites
VE-29			Reddish	Yes	2nd half of 15th	Pb intermediate (V1-4)	Thinner, poor in crystallites
VE-14	Bright light green V3		Whitish		1st half of 15th	Pb rich + Cu (V3)	Thinner, poor in crystallites
VE-17			Whitish		1st half of 15th	Pb rich + Cu (V3)	Thinner, poor in crystallites
VE-27			Reddish	Yes	1st half of 15th	Pb rich + Cu (V3)	Thinner, poor in crystallites
VE-33			Reddish	Yes	2nd half of 15th	Pb rich + Cu (V3)	Thinner, poor in crystallites
VE-36			Reddish	Yes	2nd half of 15th	Pb rich + Cu (V3)	Thinner, poor in crystallites
VE-23	Dark green V6		Reddish		End of 14th	Pb poor (V6)	Thicker, rich in crystallites
VE-24			Reddish		End of 14th	Pb poor (V6)	Thicker, rich in crystallites
VE-25			Reddish		End of 14th	Pb poor (V6)	Thicker, rich in crystallites
VE-29	Honey V9		Reddish		2nd half of 15th	Pb intermediate (V1)	Thinner, poor in crystallites

with distilled water to remove the adhered soil and to prevent glaze damage.

The potsherds were cut crosswise to obtain a polished thin section that included the glaze and the ceramic

body. Microscopic observations of the glaze layer and its relationship with the body were performed using a polarizing Nikon Eclipse LV100POL microscope with a DS F-11 digital camera.

2.3 | Scanning electron microscopy

Electron microscope studies of the glazes were performed on carbon-coated polished thin sections in order to examine the glaze microstructure, the glaze-ceramic body interface, and to determine the type of colouring agent and the elemental composition of the glaze. Scanning electron microscopy combined with energy-dispersive X-ray spectrometric analysis (SEM-EDX) used a JEOL JSM-6400 scanning electron microscope, coupled with an Oxford Pentafet photon energy instrument with a Link Isis X-ray (EDX) microanalysis system. The backscattered electron resolution was 3 nm at 15 kV and 10 mm working distance. The analytical data were obtained by INCA software. The EDX measurements were conducted at 20 kV accelerating voltage with a collecting time of 300 s. Measurements were taken on different areas of the same glaze on each piece. Twelve diagnostic element oxides were considered (PbO, Si₂O, TiO₂, Al₂O₃, Fe₂O₃, MgO, MnO, CaO, K₂O, Na₂O, ZnO, and CuO). The chemical data were subjected to multi-dimensional principal component analysis (PCA) to establish chemical groups. Besides, backscattered electron images (BSE) were obtained to observe the characteristics of glazes and the body/glaze interface.

2.4 | Raman spectroscopy

The Raman spectroscopic analyses of the glazes were performed both directly on the cross section of the glazed surface and on polished thin sections. A micro-Raman spectroscope with a Renishaw InVia Raman spectrometer coupled with a Leica DMLM microscope, with a spatial resolution of 1–2 μm for the ×50 objectives was used. For quality assurance of the spectra, daily calibration was performed using the 520.5 cm⁻¹ Raman band of a silicon chip. A laser of 514 nm (ion-argon laser, Modu-Laser) and a holographic net of 1800 lines/mm were used. For each spectrum, 20 s was employed, and five scans were accumulated, with a laser power lower than 2 mW, in the spectral window from 150 cm⁻¹ to 1500 cm⁻¹.

The software used to collect Raman spectra was WIRE (Renishaw, UK), and the obtained spectra were processed with OMNIC (Nicolet, Madison, Wis., USA). First, background subtraction was performed using linear segments placed at the same locations and using minimal reference points (between 6 and 8) and the spectral windows recommended by authors.^[24] Background corrections removed the Boson peak (intense for lead-rich glazes) in order to obtain only the molecular information of the Si–O network. The curve-fitting was done with either Gaussian and Lorentzian functions according to

the amorphous or crystalline status of the studied glaze phases, respectively. In order to characterize the glazes, the spectral deconvolution of the Si–O stretching and bending ranges was performed for the identification of the spectral components related to Q⁰, Q¹, Q², and Q³–Q⁴. In addition, the polymerization index I_p was calculated as the ratio of the bending and the stretching envelopes (A₅₀₀/A₁₀₀₀ peak area ratio), following Colombari.^[25] The acquired Raman spectra of crystalline phases at the body/glaze interface on polished thin sections were compared with Raman spectra of pure standard compounds collected in the e-VISNICH dispersive Raman database and with RRUFF free Raman databases.

2.5 | X-ray diffraction

X-ray diffraction was used to estimate the firing temperature from the mineralogical composition of the over-fired sample body. This sample corresponds to a glazed ceramic manufactured by a single-firing process. The obtained temperature for the body was compared with the temperature obtained by Raman spectroscopy for the glaze. Mineralogy was determined on a powder sample using a Philips X'Pert diffractometer (Malvern PANalytical, Almelo, The Netherlands) equipped with graphite monochromator adjusted to Cu-k_{α1} X-radiation operating at 40 kV and 20 mA. The data collection was performed in a continuous scan ranging from 5 to 70°2θ at acquisition rate of 0.02°2θ per second. The mineral phase identification was performed using X'Pert HighScore Plus 3.0 software (Malvern PANalytical, Almelo, The Netherlands).

3 | RESULTS AND DISCUSSION

3.1 | Optical microscopy observations

Defining the colour of the glaze on all ceramic sherds was not always easy since chromatic gradations on the same surface are frequent. The dark-green colour of the V6 glaze was the most common colour until the second half of the 15th century. From the second half of the 15th century ceramics with two-sided coloured glazes became more common although the first cases were found at the end of the 14th century. On some fragments V1 yellow-honey on the inside and V3 light green on the outside was observed. Therefore, there was no chronological relation in the usage of particular glaze colours. Glazes of V0, V6 and V9 glaze colours were applied on reddish ceramic bodies and whereas V1 on the whitish bodies. Besides, an underglaze white slip was observed for V3 glazes and for

some pieces with V1 glazes. The slip was used to cover the reddish ceramic body and provide a white background to highlight the honey and light green colour of the glazes (Table 1).

Optical observations of the glazes in thin sections show that they are very clean without mineral inclusions and bubbles. The glaze and body boundaries are generally sharp and clearly-defined as for V0, V1 and V3 glazes. Whereas the boundaries for V6 and some samples of V1 glazes exhibit a fuzzier limit (Figure S1). Tiny needle crystallites are observed at the seamless boundary of V6 and some V1 glazes with the body. The case of the V1 glaze is remarkable, where three different situations were observed, with slip and a net boundary, and without slip and with boundaries both net and undefined. In plane-polarized light mode V0 and V9 glazes display a light yellow colour; V1 glaze is pink and V6 is a transparent beige colour; while V3 glazes vary from light green to deeper green.

3.2 | Scanning electron microscopy

The glaze and the body/glaze and slip/glaze interfaces were investigated by SEM-EDX. The results indicate that

glazes are clean with scarce or rare residual minerals and gas bubbles, and they are well preserved and with no signs of weathering (Figure 1). Sometimes scarce residual quartz or potassium feldspar inclusions (grain size 10–50 μm) are observed. The body/glaze or slip/glaze interfaces are mainly thin except for V6 and some V1 glazes with a wider reaction interface with abundant growth of tiny crystallites (Figure S2). The glazes are usually poorly fractured although some large cracks perpendicular to the ceramic surface, due to shrinkage during cooling or when removing from the kiln, are sometimes observed.^[21] The glazes display a homogeneous thickness ranging between 50 and 120 μm although sometimes thicker glazes of up to 200 μm are observed in holes or curved zones.

The chemical results of EDX analysis of different glazes are listed in supplementary Table S1. The EDX analysis of several areas of the same glaze shows lead to be the most abundant compound. The lead content varies between 36.2 wt% and 64.2 wt%, the silica content between 27.3 wt% and 46.9 wt%, and the alkali content ($\text{Na}_2\text{O} + \text{K}_2\text{O}$) is lower than 2 wt%. Thus, all the studied glazes can be considered lead glazes.^[11] The iron concentration ranges between 2 wt% and 5 wt% except for V3 glazes with 1.3 wt%. Iron was used as a colouring agent

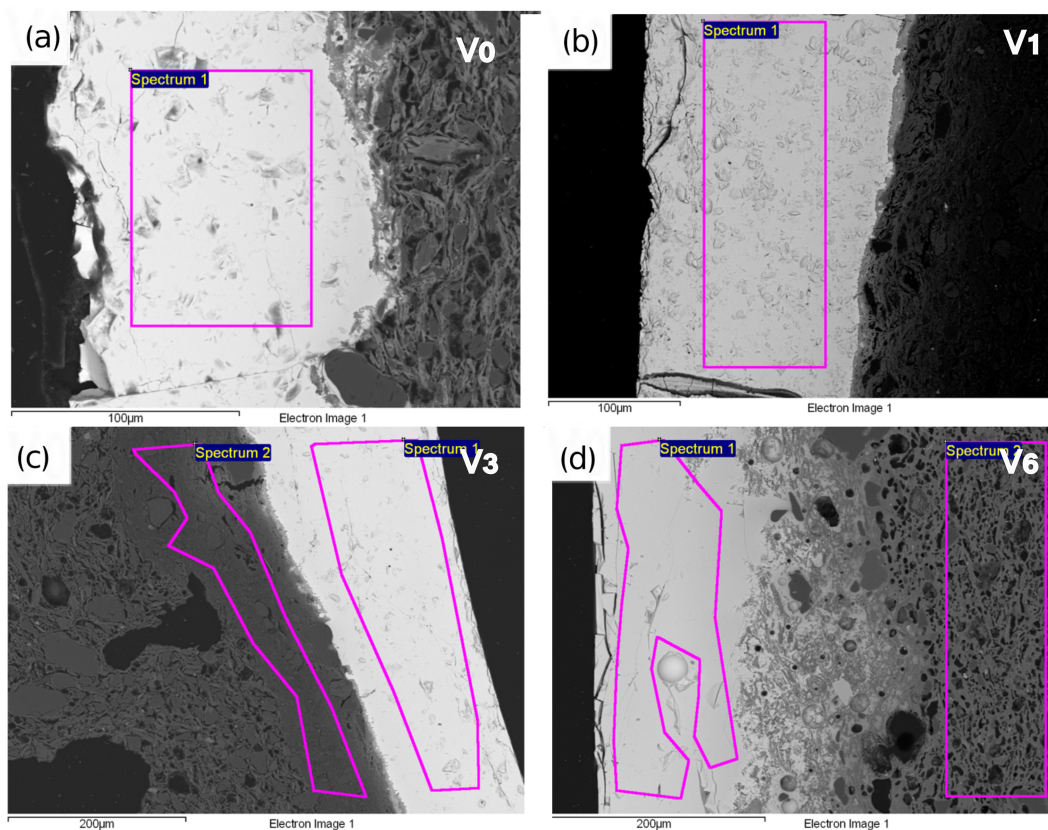


FIGURE 1 SEM backscattered electron photomicrographs of the different types of glazes: (a) honey-marbled V0 glaze, (b) honey yellow V1 glaze, (c) bright light green V3 glaze on the white slip, and (d) dark green V6 glaze. The delimited areas correspond to analysed zones [Colour figure can be viewed at wileyonlinelibrary.com]

for most of the glazes under oxidizing firing conditions while copper was employed for V3 glazes.

Principal component analysis (PCA) was carried out on SEM-EDX chemical data of the glazes (Figure 2). The first two components account for 71% of the variance. PC1 positive values are influenced by calcium and iron, and negative values by lead. PC2 positive values are influenced by copper and aluminium, and negative values by zinc. PCA analysis discriminated two main groups: lead-poor, such as V6 glazes; lead-rich glazes including V3 and V0; and between both groups (rich/poor lead glazes) such as V9 glazes. The chemical characteristics of V1 glazes discriminate four subgroups: V1-1, V1-2, V1-3 and V1-4. V1-1 are lead-rich glazes, the V1-2 are zinc-rich and lead-rich glazes, V1-3 are zinc-and calcium rich and lead-poor glazes, and V1-4 glazes are lead-rich similar to V9 glazes with moderate content on calcium and enriched in aluminium. In addition, V1-1, V3 and V6 glazes are rich in aluminium.

The SEM-EDX results indicate that at least five recipes were used for the production of the glazes, starting with two basic types of fluxes, one lead rich and one lead poor. Specific metallic oxides were added to these fluxes to obtain the specific characteristics and the desired colours.

The bright light green colour of V3 glazes was obtained by adding copper (Cu^{+2}) as a colouring agent.^[26–28] In contrast, iron was responsible for the dark green colour of V6 glazes applied over a reddish clay body in a single firing process. Iron oxides also acted as glaze colourant for the honey-yellow V1, honey-marbled V0 and the honey-coloured V9 glazes commonly applied over a reddish clay body. Thus, the employment of the white slip between the ceramic body and the glaze enhanced the glaze brightness and widened the chromatic range of ceramics. Besides, the honey-yellow V1-2

and V1-3 glazes are characterized by the addition of zinc which improves glaze stability and resistance, and contributes to the conservation of the glaze colour and brightness.^[29,30]

The metal transition elements (Fe, Cu, ...) were probably obtained from raw minerals such as haematite (Fe_2O_3), and azurite and malachite ($\text{Cu}_3(\text{CO}_3)_2(\text{OH})_2$ and $\text{Cu}_2\text{CO}_3(\text{OH})_2$, respectively). The provenance area for these raw minerals could be the nearby mining area of the Sierra de la Demanda (Burgos) where iron ores and other metallic minerals such as lead-zinc, copper, manganese, and silver have been exploited since ancient times.^[31]

The body/glaze or slip/glaze interfaces were investigated by SEM to obtain data about the production technology of the glazes (Figures 2 and S2). The morphology of the interface is related to the manufacturing technology, thus providing information on the firing process and chemical composition of the body and glaze.^[11,32–34] The studied glaze interfaces are mainly thin although wider interfaces were observed in some cases. Thin interfaces $<15\ \mu\text{m}$ (Figures 2a–c and S2a–c) are observed for V0, most of V1, V9 and V3 glazes with occasional new formed crystallites. The scarcity of raw material mineral inclusions within these glazes, the absence of bubbles and the scarcity of newly formed crystallites suggest that glazes were probably applied on previously fired bodies or bodies + slips, indicating a double-firing process.^[32,33] In contrast, the interfaces of V6 glazes and some yellow-honey, V1-3 glazes are thicker (80–150 μm) (Figures 2d and S2d) as a result of the diffusion of the elements between the body and glaze during firing. When glazes were applied over unfired bodies, the diffusion process leads to a thicker interface, with a significant crystallization of tiny crystallites; these characteristics can be indicative of a single-firing process.^[34,35]

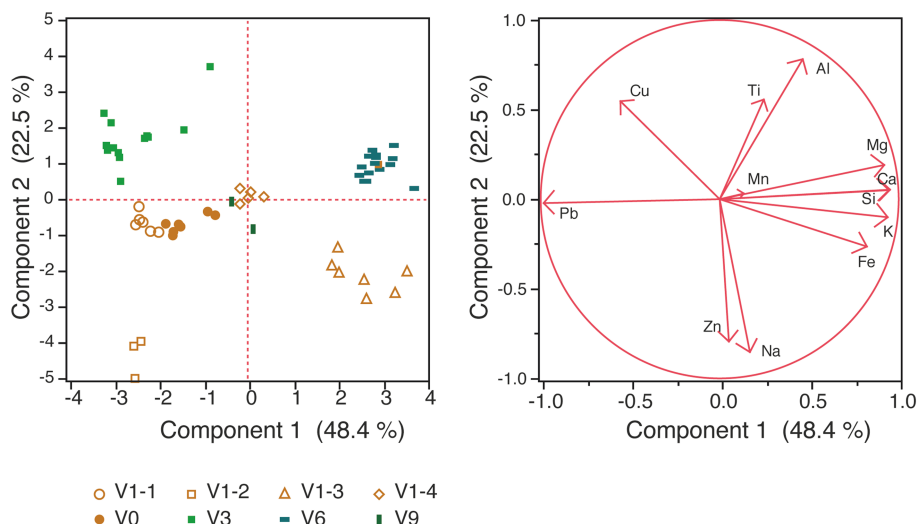


FIGURE 2 Principal component analysis of the chemical composition of the glazes using SEM-EDX chemical results [Colour figure can be viewed at wileyonlinelibrary.com]

Slip-bearing samples of V3 and most samples of V1 glazes exhibit thin slip-glaze interfaces with poor crystallites growth. In addition, the nature of the white slip was analysed by SEM-EDX, which determined its kaolinite nature, according to high aluminium and relatively low silica contents. The kaolinitic composition of the slip also prevents the extension of the interface.^[34] For ceramics with white slip, glazes were probably applied after the firing of the underlayer (body + slip), resulting in at least two firing processes.

Thus, several firing scenarios were observed in the studied ceramics. The most widespread procedure was a double firing method where ceramic bodies (with or without a slip) were fired before glazing. However, a single-firing procedure was employed especially for dark green V6 (and some V1) ceramics, where bodies and glazes were fired simultaneously. The scarcity of raw material inclusions and the transparency and the brightness of the glazes could indicate melting temperatures ranging from 750°C to 800°C.^[34,35]

3.3 | Raman spectroscopy

Raman spectroscopy was performed on the cross section of the surfaces of the bulk samples to determine glaze composition and to estimate the firing temperatures. After several attempts, Raman spectroscopy on thin sections did not provide satisfactory results since the samples gave rise to a fluorescence that interferes with Raman signals due to organic residues or inorganic impurities embedded in glazes. The glaze firing temperatures can be determined by the polymerization index, calculated as the ratio of Si–O bending and stretching mode area of the spectra at ≈ 500 and 1000 cm^{-1} , respectively.^[3,24] Considering the intensity ratio of these vibrational modes, the bulk composition of the glaze and the firing temperature were estimated.

The Raman spectra of the glazes show two broad bands with a more intense band of stretching (between 800 and 1200 cm^{-1} , maximum at 950 cm^{-1}) than the bending Si–O–Si mode envelope (maximum at 484 cm^{-1}) (Figure 3). The following three bands of Si–O stretching envelope were considered: Q^1 (in the region of 850 – 900 cm^{-1}), Q^2 (in the region of 950 cm^{-1}), and Q^3 (in the region of 1000 – 1100 cm^{-1}) (Figure 4, Table 2). However, the fitting does not work properly at low wavelength numbers. To improve the deconvolution, other components were added. At first, Q^0 was considered since the problematic wavelength numbers were at around 800 cm^{-1} , besides the separation of the Q^3 – Q^4 were considered but the deconvolution fit and residuals were not improved. The centre of gravity of Q^1 and Q^2 is a function

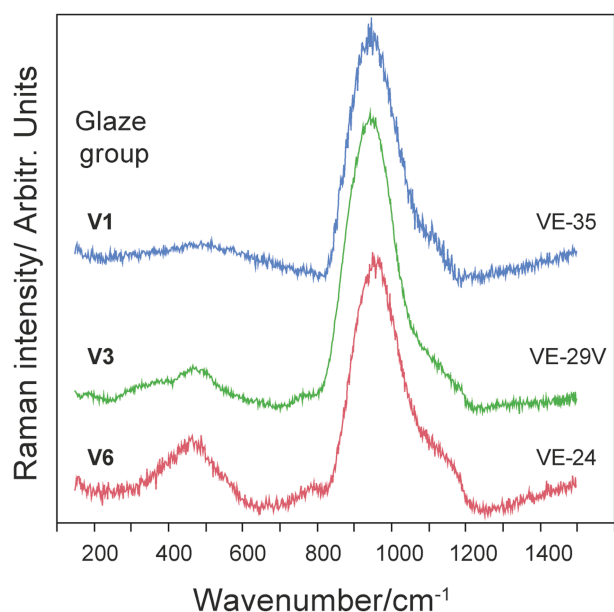


FIGURE 3 Representative Raman spectra of lead glazes including the dark green V6 glaze (VE-24 sample), bright light green V3 glaze (VE-29 sample), and honey yellow V1 glaze (sample VE-35) [Colour figure can be viewed at wileyonlinelibrary.com]

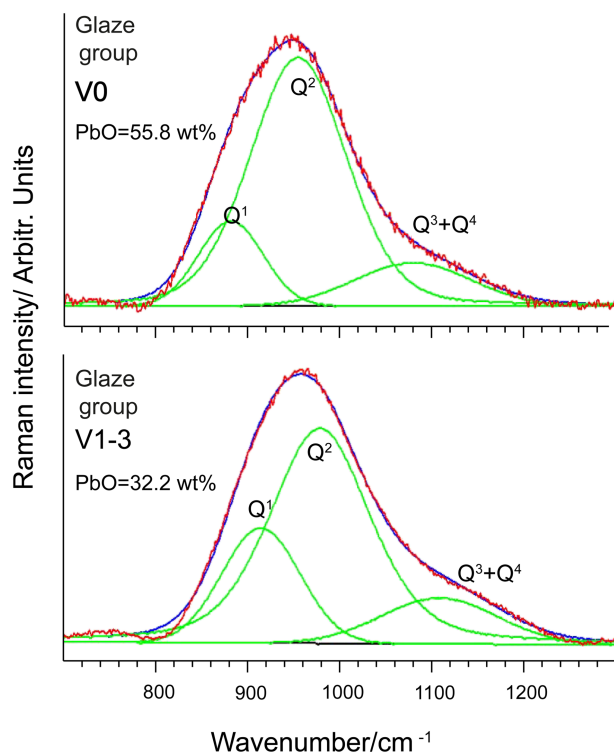


FIGURE 4 Representative Raman spectra of lead glazes and Q_n components of the Si–O stretching band [Colour figure can be viewed at wileyonlinelibrary.com]

of the composition of the glaze. The maxima of the deconvoluted bands varies in the wavenumber range of 907 – 921 cm^{-1} and 886 – 904 cm^{-1} , from low-lead (V1-3 and V6

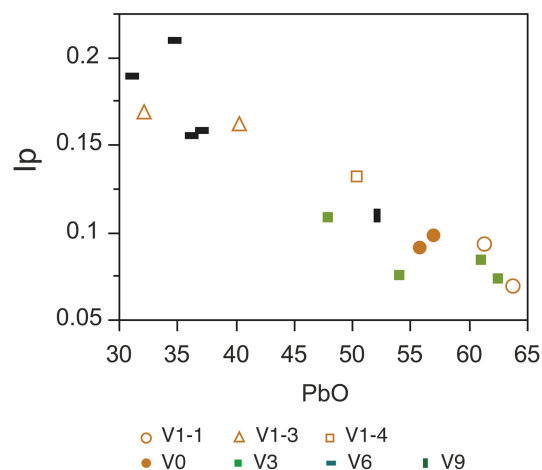
TABLE 2 Spectral position (ν , cm^{-1}) and relative intensity obtained from the deconvolution process of the glaze spectra for analysed glazes, including the glaze type, lead content (% wt.) Q_1 , Q_2 , Q_3 components of the stretching modes

Sample	Type	Pb	I_p	νQ_1	Q1 height	νQ_2	Q2 height	νQ_3	Q3 height
VE20	V0	55.8	0.091	891	1155	957	3372	1069	587
VE22	V0	57.0	0.098	886	1210	951	3508	1055	815
VE15	V1-1	61.4	0.093	904	1087	966	2687	1106	423
VE18	V1-3	40.4	0.162	913	1280	982	1798	1100	470
VE19	V1-3	32.2	0.169	918	8443	975	17,975	1095	3687
VE29MC	V1	50.4	0.132	921	1011	977	1850	1115	359
VE35	V1-1	63.8	0.069	890	9716	957	24,466	1078	3376
VE17	V3	54.1	0.075	889	10578	956	24,169	1085	4506
VE27	V3	62.5	0.073	876	8535	938	16,534	1056	4586
VE33	V3	61.0	0.084	903	8951	969	18,856	1106	2662
VE23	V6	36.3	0.155	913	769	972	1448	1105	251
VE24	V6	34.8	0.209	921	867	979	1525	1121	348
VE25	V6	37.2	0.158	916	827	975	1299	1109	321
VE36	V6	31.1	0.189	907	6121	966	12,255	1067	3898
VE29MO	V1	47.9	0.130	905	1040	969	2054	1103	338
VE29V	V9	47.9	0.200	902	386	961	894	1075	189

glazes) to high-lead content (V0, V1-2, and V3 glazes), respectively. A shift of the stretching vibration region moves towards lower wavenumbers induced by an increase in the lead content because of depolymerization of the Si-O network. The formation of a less compact structure characterizes a low polymerization index (Table 2).

The polymerization index I_p is correlated with the composition of glazes and with the firing temperature.^[24,25,36,37] The I_p index of the analysed glazes ranges between 0.073 and 0.209 (Table S2). Good correlation was observed between the I_p and the lead content of the glaze ($I_p = 0.2991528 - 0.0036152 * \text{PbO}$, $R^2 = 0.88$) (Figure 5). The I_p values lower than 0.3 are typical of high lead glazes. The highest I_p values (0.155–0.209) correspond to dark green V6 and yellow-honey V1-3 glazes showing low-lead content while lower I_p values correspond to the remaining glazes (V0, V1-1, V1-2, V3, and V9). Moreover, I_p values lower than 0.3 indicate low firing temperatures below 700°C for the glazing process.^[1,38]

However, Sample VE-36, corresponding to low-lead with a dark-green V6 glaze, shows over-fired features. X-ray diffraction analysis of the body detected diopside and a plagioclase minerals assemblage suggesting a minimum firing temperature of 900°C.^[39] Considering that the VE-36 glaze was manufactured by a single firing process and that the I_p value is 0.189, the variations in I_p are related to composition rather than to firing temperature.

**FIGURE 5** Bivariate diagram showing the polymerization index (I_p) versus PbO content of the different chemical groups of glazes [Colour figure can be viewed at wileyonlinelibrary.com]

Raman analysis performed on thin sections of V6 glazes identified pseudobrookite and rutile at the interface characterized by the bands at 200 and 227 cm^{-1} and 446 and 610 cm^{-1} , respectively (Figure S3). Pseudobrookite was mainly detected in the outmost part of the interface, away from the body, while at the interface close to the body both phases coexist. The presence of these phases was only observed in those cases of a single firing, that is, for ceramics where the body and the glaze were fired simultaneously. The coexistence of these

titanium oxides suggests firing temperatures of about 750°C.^[39]

4 | CONCLUSION

Raman spectroscopy combined with SEM-EDX analyses was able to characterize the glazes of medieval ceramics from Vega workshop (Burgos, Spain). All the glazes studied are transparent and without inclusions or crystalline phases remains. Most of them exhibit a thin body/glaze or slip/glaze interface, except for the dark green V6 and some V1-3 glazes that show a wider interface with acicular crystallites. The characteristics of these interfaces indicate different firing procedures: from a single firing process for the ceramics with the V6 and some V1-3 glazes to two or more firing processes for rest of the glazes. To obtain the different colours of the glazes, not only specific metallic oxides were used but also the use of a white slip, which increased the colour palette and enhanced the glaze colour depth.

The SEM-EDS and Raman results indicate that all the studied glazes correspond to lead glazes. The polymerization index values (I_p) are related more closely to the chemistry of the glaze than to the firing temperature. The low polymerization indexes (<0.21) suggest firing temperatures lower than approximately 750°C for all the glazes. However, the XRD data of the overfired VE-36 ceramic, questioned the use of the I_p parameter to estimate firing temperatures. The occurrence of a pyroxene-plagioclase assemblage indicates firing temperatures over 900°C even though the I_p values of the VE-36 ceramic is 0.19. In contrast, the coexistence of pseudobrookite and rutile in the interface of single-fired V6 glaze ceramics suggests firing temperatures of about 750°C.

ACKNOWLEDGEMENTS

This study was partially supported by the IT1193-19 Research Group of the Basque Country Government and by Cronos S.C. (Burgos). The petrographic analyses of the thin sections were performed by the authors at the University of the Basque Country. The SEM-EDX and Raman spectroscopy analyses were performed at the Materials and Surface Unit Laboratory and the Raman-LASPEA Laboratory in the Advanced Research Facilities (SGIker) of the University of the Basque Country (UPV/EHU).

DATA AVAILABILITY STATEMENT

Data available on request from the authors.

ORCID

Ainhoa Alonso-Olazabal  <https://orcid.org/0000-0002-6994-0098>

Luis Angel Ortega  <https://orcid.org/0000-0002-8929-0328>

Maria Cruz Zuluaga  <https://orcid.org/0000-0003-1290-4093>

REFERENCES

- [1] P. Colomban, G. March, L. Mazerolles, H. Binous, N. Ayed, H. Slim, *J. Raman Spectrosc.* **2003**, *34*, 205.
- [2] P. Colomban, O. Paulsen, *J. Amer. Ceram. Soc.* **2005**, *88*, 390.
- [3] P. Colomban, F. Treppoz, *J. Raman Spectrosc.* **2001**, *32*, 93.
- [4] P. McMillan, B. Piriou, *Bull. Mineral.* **1983**, *106*, 57.
- [5] P. Colomban, A. Slodzyck, *Opt. Mater.* **2009**, *31*, 1759.
- [6] L. D. Kock, D. DeWaal, *Spectrochim. Acta Part A Mol. Biomol. Spectrosc.* **2008**, *71*, 1348.
- [7] D. Bikiaris, S. Daniilia, S. Sotiropoulou, O. Katsimbiri, E. Pavlidou, A. P. Moutsatsou, Y. Chrysoulakis, *Acta Part A Mol. Biomol. Spectrosc.* **1999**, *56*, 3.
- [8] P. Colomban, R. De Laveaucoupet, V. Milande, *J. Raman Spectrosc.* **2005**, *36*, 829.
- [9] M. A. Legodi, D. De Waal, *Spectrochim. Acta Part A Mol.* **2007**, *66*, 135.
- [10] L. Robinet, C. Coupry, K. Eremin, *J. Raman Spectrosc.* **2006**, *37*, 789.
- [11] M. S. Tite, I. Freestone, R. Mason, M. Molera, M. Vendrell-Saz, N. Wood, *Archaeom.* **1998**, *40*, 241.
- [12] J. Molera, J. C. C. López, G. Molina, T. Pradell, *J. Archaeol. Sci. Rep.* **2008**, *21*, 1141.
- [13] P. Colomban, *Raman Spectroscopy in Archaeology and Art History*, The Royal Soc Chemist, RSD, London **2019** 1.
- [14] M. C. Zuluaga, A. Alonso-Olazabal, M. Olivares, L. Ortega, X. Murelaga, J. J. Bienes, A. Sarmiento, N. Etxebarria, *J. Raman Spectrosc.* **2012**, *43*, 1811.
- [15] S. Coentro, R. C. da Silva, C. Relvas, T. Ferreira, J. Mirão, A. Pleguezuelo, R. Trindade, V. S. F. Muralh, *Microsc. Microanal.* **2018**, *24*, 300.
- [16] Q. Ma, S. Xu, J. Wang, J. Yan, *Mater. Chem. Phys.* **2020**, *242*, 122213.
- [17] J. Molera, T. Pradell, N. Salvadó, M. Vendrell-Saz, *J. Am. Ceram. Soc.* **1999**, *82*, 2871.
- [18] I. Garofano, M. D. Robador, J. L. Pérez-Rodríguez, J. Castaing, C. Pacheco, A. Duran, *J. Eur. Ceram. Soc.* **2015**, *35*, 4307.
- [19] C. De Vito, L. Medeghini, S. Mignardi, F. Coletti, *J. Eur. Ceram. Soc.* **2017**, *37*, 1779.
- [20] J. Zamek, *Ceram. Mon.* **1995**, *43*, 82.
- [21] B. Velde, I. Druc, *Archaeological Ceramic Materials: Origin and Utilization*, Springer, Berlin **1999**.
- [22] J. García Rosselló, *Mayurqa* **2008**, *32*, 119.
- [23] D. Albero Santacreu, *Materiality, techniques and society in pottery production: the technological study of archaeological ceramics through paste analysis*, De Gruyter, Berlin **2014**.
- [24] P. Colomban, A. Tournie, L. Bellot-Gurley, *J. Raman Spectrosc.* **2006**, *37*, 841.
- [25] P. Colomban, *J. Non-Crystal Sol.* **2003**, *323*, 180.
- [26] A. Silvestri, S. Tonietto, F. D. D'Acipito, G. Molin, *J. Cult. Herit.* **2012**, *13*, 137.
- [27] E. Ozel, S. Turan, *J. Eur. Ceram. Soc.* **2003**, *23*, 352.
- [28] B. Carasu, S. Turan, *J. Eur. Ceram. Soc.* **2002**, *22*, 1447.
- [29] J. M. Fernández Navarro, *El vidrio*, CSIC, Madrid **2003**.

- [30] R. Casasola, J. M. Rincón, M. Romero, *J. Mater. Sci.* **2012**, *47*, 553.
- [31] J. A. Ibáñez Gómez, *Estudio Metalogénético de las mineralizaciones de plomo, zinc y cobre en el Paleozoico de la Sierra de la Demanda (La Rioja, Burgos)*, UPV/EHU, Leioa **1998**.
- [32] M. Walton, M. Tite, *Archaeom* **2010**, *52*, 733.
- [33] E. Palamara, N. Zacharias, M. Xanthopoulou, Z. Kasztovszky, I. Kovács, D. Palles, E. I. Kamitsos, *Microchem. J.* **2016**, *129*, 137.
- [34] J. Molera, T. Pradell, N. Salvadó, M. Vendrell-Saz, *J. Am. Ceram. Soc.* **2001**, *84*, 1120.
- [35] J. Molera, T. Pradell, S. Martínez-Manent, M. Vendrell-Saz, *Appl. Clay Sci.* **1993**, *7*, 483.
- [36] P. Colomban, M. P. Etcheverry, M. Asquier, M. Bounichou, A. Tournié, *J. Raman Spectrosc.* **2006**, *37*, 614.
- [37] P. Colomban, A. Tournié, L. Bellot-Gurlet, *J. Raman Spectrosc.* **2006**, *37*, 841.
- [38] P. Colomban, W. Milande, L. Le Bihan, *J. Raman Spectrosc.* **2004**, *35*, 527.
- [39] W. A. Deer, R. A. Howie, J. Zussman, *An introduction to the rock-forming minerals*, Mineral. Soc. Great Britain and Ireland, London **2013**.

SUPPORTING INFORMATION

Additional supporting information may be found in the online version of the article at the publisher's website.

How to cite this article: A. Alonso-Olazabal, L. A. Ortega, M. C. Zuluaga, C. Alonso-Fernández, J. Jimenez-Echevarría, A. Sarmiento, *J Raman Spectrosc* **2022**, *53*(6), 1204. <https://doi.org/10.1002/jrs.6328>